HHS Public Access

Author manuscript

Br J Pharmacol. Author manuscript; available in PMC 2022 January 19.

Published in final edited form as:

Br J Pharmacol. 2021 August ; 178(16): 3220–3234. doi:10.1111/bph.15209.

2-Hydroxypropyl-β-cyclodextrin reduces retinal cholesterol in wild type and *Cyp27a1*$^{-/-}$*Cyp46a1*$^{-/-}$ mice with deficiency in the oxysterol production

Nicole El-Darzi, **Natalia Mast**, **Alexey M. Petrov**[1], **Irina A. Pikuleva**

Department of Ophthalmology and Visual Sciences, Case Western Reserve University, Cleveland, OH USA

Abstract

Background and Purpose: 2-Hydroxypropyl-β-cyclodextrin (HPCD) is an FDA approved vehicle for drug delivery and an efficient cholesterol-lowering agent. HPCD was proposed to lower tissue cholesterol *via* multiple mechanisms including those mediated by oxysterols. CYP27A1 and CYP46A1 are the major oxysterol-producing enzymes in the retina that convert cholesterol to 27- and 24-hydroxycholesterol, respectively. We investigated whether HPCD treatments affected the retina of wild type and *Cyp27a1*$^{-/-}$*Cyp46a1*$^{-/-}$ mice that do not produce the major retinal oxysterols.

Experimental Approach: HPCD administration was either by i.p., p.o. or s.c. Delivery to the retina was confirmed by angiography using the fluorescently labeled HPCD. Effects on the levels of retinal sterols, mRNA, and proteins were evaluated by GC-MS, qRT-PCR, and label-free approach, respectively.

Key Results: In both wild type and *Cyp27a1*$^{-/-}$*Cyp46a1*$^{-/-}$ mice, HPCD crossed the blood-retinal barrier when delivered i.p. and lowered the retinal cholesterol content when administered p.o. and s.c. In both genotypes, oral HPCD treatment affected the expression of cholesterol-related genes as well as the proteins involved endocytosis, lysosomal function, and lipid homeostasis. Mechanistically, liver X receptors and the altered expression of *Lipe* (hormone-sensitive lipase), *Nceh1* (neutral cholesterol ester hydrolase 1), and NLTP (non-specific lipid-transfer protein) could mediate some of the HPCD effects.

Conclusions and Implications: HPCD treatment altered retinal cholesterol homeostasis and is a potential therapeutic approach for the reduction of drusen and subretinal drusenoid deposits, cholesterol-rich lesions and hallmarks of age-related macular degeneration.

Correspondence to: Irina Pikuleva, Department of Ophthalmology and Visual Sciences, Case Western Reserve University, 2085 Adelbert Rd., Room 303, Cleveland, OH 44106, USA. iap8@case.edu.

[1]Current affiliations: Laboratory of Biophysics of Synaptic Processes, Kazan Institute of Biochemistry and Biophysics, Federal Research Center “Kazan Scientific Center of RAS”, 2/31 Lobachevsky Street, box 30, 420111, Kazan, Russia; and Institute of Neuroscience, Kazan State Medial University, 49 Butlerova Street, 420012, Kazan, Russia

AUTHOR CONTRIBUTIONS

All the authors participated in the research design and data analysis. N.E-D. and N.M. carried out the experiments. I.A.P. wrote the manuscript.

CONFLICT OF INTEREST

The authors declare no conflict of interest.

Keywords

2-hydroxypropyl-β-cyclodextrin; retina; cholesterol; age-related macular degeneration

1 Introduction

2-Hydroxypropyl-β-cyclodextrin (HPCD) is a cyclic oligosaccharide and one of the compounds, which are shaped as hollow truncated cones composed of glycopyranose units (Coisne et al., 2016; Ohtani et al., 1989; Rosenbaum et al., 2010). The inner surface of these cones is lipophilic and the outer surface is hydrophilic, hence cyclodextrins can encapsulate hydrophobic molecules and form water-soluble inclusion complexes (Pitha et al., 1988). The size of the cavity varies amongst cyclodextrins, which affects their affinity for hydrophobic molecules (Ohtani et al., 1989). Encapsulation by a cyclodextrin changes the physico-chemical properties of a hydrophobic molecule by enhancing its solubility, stability, and bioavailability (Uekama et al., 1998).

HPCD has a relatively high affinity for cholesterol in comparison to other lipids (Christian et al., 1997; Ohtani et al., 1989) and is safe and well tolerated by mammals (Gould & Scott, 2005; Irie & Uekama, 1997). HPCD does not cross the blood-brain barrier (Calias, 2017) and has been approved by the FDA as a formulation vehicle. HPCD is currently even being tested off-label in a clinical trial (NCT01747135) for the treatment of Niemann-Pick Type C1 disease, a lysosomal cholesterol storage disorder. HPCD was also shown to be effective in both preventing and treating atherosclerosis in *Apoe*$^{-/-}$ mice by decreasing the atherosclerotic plaque size and cholesterol load (Zimmer et al., 2016). Yet, HPCD has not yet been investigated for the possibility of a cholesterol lowering effect in the retina, a multilayered sensory organ lining the back of the eye. To this date, retinal evaluations of cyclodextrins have only included intravitreal injections of methyl β-cyclodextrin to *Abca4*$^{-/-}$*Rdh8*$^{-/-}$ mice to reduce lipofuscin, a byproduct of the visual cycle (Nociari et al., 2014), as well as topical HPCD administrations to the eyes of aging C57BL/6 and mature *Cfh*$^{-/-}$ mice to lower the retinal amyloid β content and inflammation (Kam et al., 2015).

Cholesterol is a significant component of drusen and subretinal drusenoid deposits, the hallmarks of age-related macular degeneration (AMD), a cause of visual loss in the elderly in industrialized countries (Curcio et al., 2001; Curcio et al., 2005; Oak et al., 2014; Wong et al., 2014). Numerous cholesterol-related genes have been identified as risk factors for AMD (Miller, 2013). Treatment with statins, drugs which lower serum cholesterol, was shown to reduce the progression of AMD in certain patient populations (Guymer et al., 2013; Vavvas et al., 2016). Thus, retinal cholesterol targeting could be a therapeutic approach for the treatment of AMD. Hence, herein we focused on HPCD and administered the drug p.o. and s.c. to wild type (WT) and *Cyp27a1*$^{-/-}$*Cyp46a1*$^{-/-}$ mice. The latter lacking CYP27A1 and CYP46A1, the two major cholesterol-metabolizing enzymes in the retina (Mast et al., 2011), which convert cholesterol to 27- (27HC) and 24-hydroxycholesterol (24HC), respectively. *Cyp27a1*$^{-/-}$*Cyp46a1*$^{-/-}$ mice had almost a two-fold increase in the retinal cholesterol content (Saadane et al., 2014b) as well as impaired signaling *via* the liver X receptors (LXR) (Saadane et al., 2019), which are activated by 27HC and 24HC

(Janowski et al., 1999). LXRs could mediate some of the HPCD effects (Figure 1), therefore we tested whether HPCD shows efficacy in mice with normal retinal cholesterol content and an operative LXR signaling as well as in animals with an increased retinal cholesterol content and impaired LXR signaling.

2 METHODS

2.1 Animals

Female and male mice 3–5 months of age were used. WT mice on the C57BL/6J;129S6/SvEv (RRID:MGI:5654470) background and *Cyp27a1*$^{-/-}$*Cyp27a1*$^{-/-}$ mice on the C57BL/6J; 129S6/SvEv background were generated from *Cyp27a1*$^{-/-}$ (RRID:IMSR_JAX:009106) and *Cyp46a1*$^{-/-}$ (RRID:MGI:2669517) as described (Saadane et al., 2014a). All animals were free of the *Crbl*^{rd8} mutation. Mice were maintained on a standard 12-h light (~10 lux)-dark cycle and were provided regular rodent chow and water *ad libitum*. All animal experiments were approved by Case Western Reserve University's IACUC and conformed to recommendations of the American Veterinary Association Panel on Euthanasia. Littermates were selected from the pool of all available animals and randomly assigned to either the control or treatment group, which were matched by size, age (4 ± 1 month old), and gender. Sample size was based on previous experience. Investigators were not blinded with respect to mouse genotype or HPCD treatment. WT and *Cyp27a1*$^{-/-}$*Cyp46a1*$^{-/-}$ mice can easily be discriminated phenotypically as the latter are usually smaller. Two investigators, who were involved in animal treatments, were also involved in subsequent retinal isolations and assessments. These assessments (except fluorescein angiography, FA) were quantitative. Hence data analysis should not be affected by investigators's bias as all data were used and apparent outliers were not excluded.

2.2 FA

A bolus i.p. injection was used as oral administration does not provide high quality retinal images and reflects the typical FA phases (Hara et al., 1998; Squirrell et al., 2005; Watson & Rosen, 1990). Either 6-deoxy-6-[(5/6)-fluoresceinylthioreido]-HPCD (FITC-HPCD, CYCLOLab, #CY-F-2005.1, ~4.1 molar substitution for the 2-hydroxypropyl group, ~0.7 molar substitution for the fluorofore group, average Mw ~1,134) or HPCD (Millipore-Sigma, #332607, ~0.8 molar substitution for the 2-hydroxypropyl group, average Mw ~1,460) were injected at a 0.04 g/kg body weight (BW) dose. Formally, FITC-HPCD is another chemical entity. Nevertheless, because of the composite nature of all HPCDs (high number of regio- and structural isomers), we considered the fluorophore-labeled and regular HPCD as near identical molecular entities. Also, like HPCD, FITC-HPCD cannot cross the plasma membranes but can be taken up by endocytosis (Huang et al., 2016; Reti-Nagy et al., 2015). At specific time points, mice were anesthetized *via* an i.p. injection of 80 mg/kg BW ketamine and 15 mg/kg BW xylazine (Patterson Veterinary, 07-890-85598 and 07-808-1947, respectively) dissolved in sterile water. Mouse retina was imaged by a scanning laser ophthalmoscope (Spectralis HRA+OCT, Heidelberg Engineering) using a blue line of a solid state laser (488 nm).

2.3 HPCD administration

Mice were treated with HPCD either by oral gavage, daily for 11 days, or by s.c. injections twice or thrice per week for 14 or 29 days. Oral gavage models the most common drug dosing method in humans, namely when drugs are taken by mouth. However, the bioavailability of drugs administered orally may be limited as the drug will be delivered initially to the liver before its target site. In contrast, s.c. injections usually lead to a higher drug bioavalability. This is because after injection, a drug moves into the blood or lymphatic vessels and is delivered to different organs *via* the bloodstream bypassing the liver. Yet, s.c. injections are less convenient (Turner et al., 2011). For oral gavage, 20% aqueous HPCD was given to mice at a 1.6 g/kg BW dose. For the s.c. delivery, 20% aqueous HPCD was injected to mice either at a 2 g/kg BW or 4 g/kg BW dose. Control animals received similar amounts of sterile water. HPCD administration was routinely done in the morning.

2.4 Lipid quantifications

Mice were fasted overnight and the following morning were anesthetized. Blood was withdrawn *via* cardiac puncture followed by the serum and retina isolation (Mast et al., 2011; Mast et al., 2010). Sterol content (total and unesterified, the former representing a sum of the esterified and unesterified sterol) was measured as described (Mast et al., 2011; Saadane et al., 2014b) by isotope dilution GC-MS using deuterated sterol analogs as internal standards. Serum triglycerides were quantified by Marshfield Labs (Marshfield Clinic).

2.5 Quantitative RT-PCR (qRT-PCR)

Mouse retina is a tiny tissue weighing ~2.4 mg and containing ~0.25 mg protein. Hence to conduct qRT-PCR for the genes of interest, we prepared for each group a sample of 8 pooled retinas, one retina from each mouse, and isolated total RNA from these pooled samples by the TRIzol Reagent (ThermoFisher Scientific, #15596026) according to the manufacturer's instructions. Subsequent RNA processing and qRT-PCR were performed as described (Petrov et al., 2019) in triplicate on an LightCycler 480 instrument (Roche Life Science) using cDNA, a pair of gene-specific primers (Suppl. Table S1), and a FastStart Universal SYBR Green Master (Rox) (Roche Diagnostics, #04913850001); *Gapdh* served as a reference gene. Changes in the relative mRNA levels were calculated by the $2^{-\Delta\Delta Ct}$ method (Pfaffl, 2001) and normalized to the gene expression in control WT mice.

2.6 Retinal proteomics

The relative protein abundance in the retina was assessed by the label-free approach as described (Saadane et al., 2018). Three biological replicates per genotype and treatment group were used, each representing a pooled sample of two retinas from different mice. Proteins with non-significant changes ($P \geq 0.05$) in abundance between the treatment groups and the corresponding controls were excluded from the proteomics analysis as are the proteins with less than 2 unique peptides per protein and less than a 1.5-fold change in their relative abundance, despite if this change was significant. Protein grouping was based on biological process as described by UniProt (UniProtKB, RRID:SCR_004426) as well as in literature.

2.7 Data and Statistical Analysis

Quantitative data were analyzed by the Mann-Whitney *U* test. The sample size (n) is indicated in each figure or figure legend. Statistical significance was defined as *, $P \leq 0.05$. In experiments that had n<5, statistics were not done, and these studies were deemed exploratory. The data and statistical analysis comply with the recommendations on experimental design and analysis in pharmacology (Curtis et al., 2018).

2.8 Nomenclature of Targets and Ligands

Key protein targets and ligands in this article are hyperlinked to corresponding entries in http://www.guidetopharmacology.org, the common portal for data from the IUPHAR/BPS Guide to PHARMACOLOGY (Harding et al., 2017), and are permanently archived in the Concise Guide to PHARMACOLOGY 2019/20 (Alexander et al., 2019).

3 RESULTS

3.1 HPCD delivery to the retina

WT and *Cyp27a1*$^{-/-}$*Cyp46a1*$^{-/-}$ mice were injected i.p. either with HPCD-FITC or HPCD and assessed for the kinetics of retinal fluorescence (Figure 2). Only injections done with the HPCD-FITC led to a detectable fluorescent signal in the retina, which was observed in both genotypes. In the inner retina, which is nourished by the intraretinal vascular network, the fluorescent signal was initially confined to the blood vessels (up to 1 hr post-injection). Yet, with time the signal started to diffuse throughout the retina so that by 4 hrs post-injection, there was essentially no difference between the fluorescence intensity in the retinal blood vessels and the tissue. By 8 hrs post-injection, no fluorescence was detected in the inner retina, suggesting that HPCD-FITC was mainly washed out. In the outer retina, which is nourished by the choroidal vascular network, the fluorescent signal was also detected and was washed out by 8 hrs post injection as well. Thus, HPCD-FITC and probably HPCD can cross the inner and outer blood-retinal barriers and are eliminated from the retina within 8 hrs.

3.2 The levels of retinal and serum lipids after HPCD treatment by oral gavage

In HPCD-treated *vs* control WT mice, the total retinal cholesterol content was decreased only by 12% (Figure 3a), while in HPCD-treated *vs* control *Cyp27a1*$^{-/-}$*Cyp46a1*$^{-/-}$ mice, the decrease was more substantial, by 44%, with the total retinal cholesterol levels becoming comparable to that in the WT retina. The products of cholesterol metabolism by CYP46A1 (24HC) and CYP27A1 (5-cholestenoic acid, 27COOH, and 7α-hydroxy-3-oxo-4-cholestenoic acid, 7αHCA; both are generated by CYP27A1 from 27HC) were measured as well and were only detected in the WT but not the *Cyp27a1*$^{-/-}$*Cyp46a1*$^{-/-}$ retina (Figure 3b). Statistical analyses for changes in the levels of 24HC, 27COOH, and 7αHCA were not carried out as these unique measurements were conducted only on three samples for each group with each sample representing 6 pooled retinas from 6 mice. Nevertheless, it seemed that the HPCD treatment did not alter the levels of 24HC and 27COOH, while slightly increasing the levels of 7αHCA in the WT retina. While this increase is “potential” and requires further validation, it is consistent with an increase in cellular cholesterol

metabolism following HPCD treatment (Liu et al., 2009) and our previous finding that CYP27A1 is the major cholesterol hydroxylase in the retina (Mast et al., 2011). Thus, in WT mice, HPCD p.o. likely enters retinal cells *via* endocytosis and putatively increases the availability of lysosomal cholesterol for further metabolism (Figure 1).

We quantified the retinal levels of lathosterol and desmosterol (Figure 3c), the markers of cholesterol biosynthesis in neurons and astrocytes, respectively (Pfrieger & Ungerer, 2011). HPCD treatment increased the lathosterol conent in both WT and *Cyp27a1*$^{-/-}$*Cyp46a1*$^{-/-}$ retina and desmosterol content in the *Cyp27a1*$^{-/-}$*Cyp46a1*$^{-/-}$ retina. These results suggest that increased cellular cholesterol processing in the retina of HPCD-treated mice triggered a homeostatic upregulation of the retinal cholesterol biosynthesis to maintain cholesterol around steady state levels.

In addition to the retina, we tested the serum, whose lipids could be affected by HPCD treatment (Irie et al., 1992). Neither serum cholesterol nor the triglyceride levels were changed in HPCD-treated WT, and only serum cholesterol was slightly increased in HPCD-treated *Cyp27a1*$^{-/-}$*Cyp46a1*$^{-/-}$ mice (Figure 3d,e), thus suggesting that upon oral delivery and the dose used, HPCD does not carry cholesterol and fatty acids from the plasma membranes and lysosomes (Figure 1) to the bloodstream for ultimate urinary excretion.

3.3 The levels of retinal cholesterol after subcutaneous HPCD injections

Mice on oral HPCD developed loose stools toward the end of the treatment, an uncommon side effect in humans (Amar et al., 2016). Therefore s.c. HPCD injections were evaluated (Figure 4) at a dose range, which was previously shown to be safe on mice (Liu et al., 2009; Zimmer et al., 2016). Only *Cyp27a1*$^{-/-}$*Cyp46a1*$^{-/-}$ mice were assessed as oral HPCD seemed to be more efficient in retinal cholesterol lowering when sterol levels were abnormal rather than normal (Figure 3). The largest reduction of total retinal cholesterol (by 19% and 23% in male and female mice, respectively) was achieved with the highest HPCD dose (4 g/kg/BW), the frequency of injections being 2 or 3 times per week, and the treatment duration of 14 days. Decreasing the HPCD dose to 2 g/kg BW led to the total cholesterol decreases by 10% and 19% after 18 and 29 days of treatment, respectively. Thus, similar to oral HPCD, subcutaneous HPCD also decreased retinal cholesterol excess but to a lesser extent and after a longer treatment time. Hence in our subsequent studies we assessed HPCD's effects after mouse treatment by oral gavage.

3.3 Retinal gene expression after HPCD treatment by oral gavage

Four groups of genes were quantified in an exploratory study, which was carried out on one pooled sample of 8 retinas from 8 mice per genotype and treatment group with each gene being quantified in triplicate (Figure 5). Since technical replicates cannot be used for statistical analyses, we implemented an arbitrary cut off to gain insight into gene expression differences between control WT *vs* control *Cyp27a1*$^{-/-}$*Cyp46a1*$^{-/-}$ mice or between HPCD-treated *vs* control mice of the same genotype. This arbitrary cut off was a 32% change or two times 16%, the highest SD value in our triplicate technical measurements. The first group of the assessed genes included *Srebp2* and *Hmgcr*, which are related to cholesterol biosynthesis. The HPCD treatment altered the expression of only

Srebp2 in the *Cyp27a1*$^{-/-}$*Cyp46a1*$^{-/-}$ retina and did not affect *Hmgcr* expression despite *Srepb2* encodes a transcription factor which regulates *Hmgcr*. Apparently, SREBP2 did not seem to regulate the *Hmgcr* levels in the retina of mice of both genotypes. The second group of genes included *Abca1* and *Apoe*, which are regulated by LXRs. The HPCD treatment increased the expression of both genes in the *Cyp27a1*$^{-/-}$*Cyp46a1*$^{-/-}$ retina, consistent with an increase in the retinal levels of desmosterol, also an LXR ligand (Spann et al., 2012). However, the expression of *Apoe* was decreased in the WT retina, despite the retinal levels of the LXR agonists 24HC and 27COOH appeared to be unchanged in HPCD-treated WT mice (Figure 3), and 7αHCA is not an LXR agonist (Theofilopoulos et al., 2014). Probably, there was a decrease in the levels of other ligand(s) for LXR that contributed to a decreased retinal expression of *Apoe* in the HPCD-treated WT mice. The third group of genes included *Soat1*, *Lipe*, *Lipa*, and *Nceh1*, which are related to cholesterol esterification (*Soat1*) and cholesterol ester hydrolysis (the latter three). The HPCD treatment only increased the expression of *Nceh1* in the *Cyp27a1*$^{-/-}$*Cyp46a1*$^{-/-}$ retina, despite the basal *Nceh1* expression was already increased in control *Cyp27a1*$^{-/-}$*Cyp46a1*$^{-/-}$ mice along with increased basal expression of *Lipe and Lipa*. Lastly, the fourth group included *Ldlr*, *Sr-b1*, and *Cd36*, genes for receptors that bind different lipoprotein particles. The HPCD treatment decreased the transcription of *Ldlr* in the WT retina and increased the expression of *Cd36* in the *Cyp27a1*$^{-/-}$*Cyp46a1*$^{-/-}$ retina. Notably, the basal expression of *Ldlr* and *Cd36* was decreased in the *Cyp27a1*$^{-/-}$*Cyp46a1*$^{-/-}$ retina and that of *Sr-b1* was increased. These results suggested that receptor-mediate lipid uptake could also be affected by HPCD treatment but depending on the context realized *via* different mechanisms. Of course, the data obtained require further validation by qRT-PCR using larger group sizes.

3.4 Retinal proteomics after HPCD treatment by oral gavage

In HPCD-treated *vs* control (water-treated) WT mice, 30 proteins with at least 2 unique peptides and ≥1.5-fold change in retinal abundance were identified: 12 and 18 had decreased and increased expression, respectively (Table 1). In HPCD-treated *vs* control (water-treated) *Cyp27a1*$^{-/-}$*Cyp46a1*$^{-/-}$ mice, 31 of such proteins were identified: 4 with decreased abundance and 27 with increased abundance (Table 2). Proteins affected by HPCD treatment did not overlap in the two genotypes but participated in the same biological processes: vesicular transport and cytoskeletal organization; metabolism and energy homeostasis; genetic information transfer; and protein folding. In both genotypes, changes in the abundance of these proteins could affect endocytosis, lysosomal function, and lipid homeostasis (Figure 6). In addition, HPCD treatment uniquely affected the proteins involved in the ubiquitin-proteasome system, survival and signaling in the WT retina and many crystallins in the *Cyp27a1*$^{-/-}$*Cyp46a1*$^{-/-}$ retina (Tables 1, 2). Thus, the retinal proteomics data provided insight into the specific proteins and mechanisms that lower retinal cholesterol in the WT and *Cyp27a1*$^{-/-}$*Cyp46a1*$^{-/-}$ retina.

4 DISCUSSION AND CONCLUSIONS

This work is the first, to the best of our knowledge, comprehensive evaluation of HPCD effects on mouse retina. By using a fluorescently-labeled HPCD, we first established that HPCD (i.p.) can cross the blood-retinal barrier and enter the retina (Figure 2). Then, we

showed that oral HPCD lowered the retinal cholesterol content when sterol levels were normal (in WT mice) and elevated (in *Cyp27a1*$^{-/-}$*Cyp46a1*$^{-/-}$ mice) (Figure 3). In addition, we found changes in the levels of other retinal sterols (Figure 3), thus suggesting that HPCD altered retinal cholesterol homeostasis. Next, we compared different routes of HPCD delivery and used *Cyp27a1*$^{-/-}$*Cyp46a1*$^{-/-}$ mice as a model of an increased retinal cholesterol content. This comparison revealed that the retinal cholesterol reduction was higher in oral HPCD administration than in s.c. injections (Figure 4). Hence subsequent mechanistic studies were conducted on animals which received HPCD by oral gavage.

The quantifications of the retinal gene expression suggested that in *Cyp27a1*$^{-/-}$*Cyp46a1*$^{-/-}$ mice, the retinal HPCD effects were likely realized, at least in part, *via* the LXR-dependent mechanism as the expression of both *Abca1* and *Apoe*, the LXR target genes, was increased in the treated group (Figure 5). However, such an effect was not observed in the retina of HPCD-treated WT mice, likely because their retinal cholesterol levels were normal prior to HPCD treatment. Hence the homeostatic response to HPCD treatment was perhaps to retain these levels by reducing cellular cholesterol efflux on the APOE-containing lipoprotein particles. In contrast, in the *Cyp27a1*$^{-/-}$*Cyp46a1*$^{-/-}$ mice, the retinal cholesterol levels were significantly elevated prior to HPCD treatment. Therefore the homeostatic response was to lower these levels and increase cholesterol output *via* reverse cholesterol transport mediated by *Abca1* and *Apoe*. Remarkably, the LXR-dependent regulation was still operative in the *Cyp27a1*$^{-/-}$*Cyp46a1*$^{-/-}$ retina, which does not produce 27HC and 24HC, the oxysterol ligands for LXRs. Yet, the retinal levels of desmosterol, another LXR ligand, were increased (Figure 3c) and could lead to an increase in the LXR-dependent gene transcription.

Sterol quantifications revealed that the cholesterol ester hydrolysis was increased upon HPCD treatment (Figure 3a), whereas the gene expression studies pointed to the specific enzymes that could hydrolyze cholesterol esters in the retina (Figure 5). *Lipe* is the gene for ubiquitous hormone-sensitive lipase, which normally is a cytosolic protein, yet moves to the surface of lipid droplets upon lipolytic stimulation (Yeaman, 2004). *Lipa* encodes lysosomal acid lipase, the only known enzyme, which can hydrolyze cholesterol esters in the lysosomes (Li & Zhang, 2019). The gene product of *Nceh1* is the neutral cholesterol ester hydrolase 1 (or KIAA1363 in mice), a microsomal enzyme, which controls the cholesterol ester content in lipid droplets (Igarashi et al., 2010; Okazaki et al., 2008). The HPCD effects on the genes for various cholesterol ester hydrolases appeared to be context-specific, i.e. different in the WT and *Cyp27a1*$^{-/-}$*Cyp46a1*$^{-/-}$ retina. In the WT retina, HPCD administration seemed to elicit a 27% increase in the levels of *Lipe*, however this increase was still below our arbitrary cut off of 32%. Yet, in the *Cyp27a1*$^{-/-}$*Cyp46a1*$^{-/-}$ retina, the treatment increased the expression of *Nceh1* by 34% (Figure 5). We suggest that the apparent genotype-dependent upregulation of the cholesterol ester hydrolases in the retina of HPCD-treated mice (Figure 5) could be due to several reasons. One reason could be the cell-specific (in the photoreceptor outer segments) cholesterol ester accumulation in *Cyp27a1*$^{-/-}$*Cyp46a1*$^{-/-}$ mice. Alternatively or in addition, NCEH1 could be a more robust cholesterol ester hydrolase than LIPE. Therefore, *Nceh1* became upregulated in the retina of HPCD-treated *Cyp27a1*$^{-/-}$*Cyp46a1*$^{-/-}$ mice to efficiently hydrolyze large amounts of cholesterol esters present in the retinal lipid droplets of these animals (Saadane et al., 2016).

Our work brings attention to the three retinal cholesterol ester hydrolases, which need to be considered in future studies of retinal cholesterol maintenance.

The HPCD effects on the retinal expression of the genes for the lipoprotein particle receptors were similar in WT and *Cyp27a1*$^{-/-}$*Cyp46a1*$^{-/-}$ mice for *Sr-b1* and *Cd36* but not *Ldlr* (Figure 5). A significant *Ldlr* downregulation in the retina of HPCD-treated WT mice could be due to the drug's effect on receptor trafficking to the lysosomes following ligand binding and endocytosis. This explanation is suggested by the retinal proteomics analysis and is exemplified by LRP1, an LDLR-related protein, as discussed below.

The retinal proteomics analysis of the WT retina was consistent with the HPCD effects on endocytosis and Ca^{2+}-dependent exocytosis as the suggested mechanisms (Figure 1) of the cellular HPCD uptake and removal, respectively (Chen et al., 2010; Plazzo et al., 2012; Rosenbaum et al., 2010). Increased abundance of AT10A could indicate increased endocytosis, whereas decreased abundance of DMXL2 could affect HPCD removal *via* exocytosis. In addition, the lysosomal pH could be increased as well, and impair the disassembly of LDLR and LRP1 in the lysosomes. This could lead to a decreased availability of the receptor-delivered cholesterol for post-lysosomal processing and a decrease in the levels of ligand-free lysosomal LRP1 and LDLR available for recycling back to the cell surface. Consequently, this decreased recycling may decrease the delivery to the lysosomes of the cholesterol-bound receptor *via* CA2D2, which interacts with LRP1 and is at a decreased abundance. Therefore, the *Ldlr* expression and LRP1 abundance were decreased. As for the HPCD effect on the post-lysosomal cholesterol processing, increased abundance of NLTP suggests that cholesterol distribution from the lysosomes to different cellular organelles and plasma membranes could be enhanced, thus leading to increased cholesterol extraction from the plasma membranes by extracellular HPCD. In addition, increased abundance of TMED2 could increase the vesicular exchange between the endoplasmic reticulum (ER) and Golgi complex and thereby provide more cholesterol for subsequent NLTP-mediated removal.

Similar to the retina of HPCD-treated WT mice, the retina of HPCD-treated *Cyp27a1*$^{-/-}$*Cyp46a1*$^{-/-}$ mice also had altered abundance of the proteins involved in endocytosis (ARFG1, PP2BB, IQEC3) and lysosomal acidification (S4A7, CAH3, DMXL2, and CRBA1) (Figure 6). However, these were different proteins as compared to those in HPCD-treated WT mice (except for DMXL2). Therefore, we envision that cholesterol distribution from the lysosomes to different subcellular organelles was mediated by HPCD, including transport to the ER, where there was already an accumulation of cholesterol due to lack of CYP27A1 and CYP46A1. This cholesterol excess was esterified (Figure 3a) and localized to lipid droplets (Saadane et al., 2016). Hence, to compensate for an increased cholesterol delivery by HPCD to the ER and consequently increased need for cholesterol esterification, the abundance of FABP5, which transports fatty acids, was increased. This in turn, probably triggered a compensatory increase in the cholesterol ester hydrolysis by NCEH1, whose abundance was increased, possibly as a result of a decreased lipid droplet biogenesis due to increased expression of CDS2, ARFG1, CAH3, and RCN3. The free cholesterol formed was probably then transported to the plasma membranes and extracted

by extracellular HPCD. Future studies are necessary to further test the suggested putative mechanisms of the HPCD effects on the WT and *Cyp27a1*$^{-/-}$*Cyp46a1*$^{-/-}$ retina.

In conclusion, the present study provides evidence that the orally administered HPCD enters the retina and enhances endocytosis, a mechanism for cellular HPCD uptake. Lysosomal acidification, intracellular and reverse cholesterol transport, LXR-signaling, maintenance of lipid droplets, and exocytosis become affected and alter the cellular cholesterol homeostasis. Different proteins seem to mediate the HPCD effects in different genotypes, but the ultimate result is similar, i.e. a reduction in the retinal cholesterol content. Our data suggest that oral HPCD treatment should be further tested as a potential therapeutic for AMD, a disease, which is characterized by retinal cholesterol dyshomeostasis and cholesterol or cholesterol ester accumulations in specific locations. We also identified NCEH1, FABP5, and NLTP as important players in retinal cholesterol maintenance.

Supplementary Material

Refer to Web version on PubMed Central for supplementary material.

ACKNOWLEDGEMENTS

This work was supported in part by the National Institutes of Health grants EY025383, EY018383, and EY011373 and the unrestricted grant from the Cleveland Eye Bank Foundation. Irina A. Pikuleva is a Carl F. Asseff Professor of Ophthalmology. The authors thank the Visual Sciences Research Center Core Facilities (supported by the National Institutes of Health grant P30 EY11373) for assistance with mouse breeding (Heather Butler and Kathryn Franke), animal genotyping (John Denker), tissue sectioning (Catherine Doller), and microscopy (Anthony Gardella). We are also grateful to Danie Schlatzer (Proteomics and Small Molecule Mass Spectrometry Core) for conducting the retinal label free analysis.

DECLARATION OF TRANSPARENCY AND SCIENTIFIC RIGOUR

This Declaration acknowledges that this paper adheres to the principles for transparent reporting and scientific rigor of preclinical research as stated in the BJP guidelines for Design & Analysis, Immunoblotting and Immunochemistry, and Animal Experimentation and as recommended by funding agencies, publishers, and other organizations engaged with supporting research.

Abbreviations:

7αHCA	7α-hydroxy-3-oxo-4-cholestenoic acid
24HC	24-hydroxycholesterol
27COOH	5-cholestenoic acid
27HC	27-hydroxycholesterol
AMD	age-related macular degeneration
BW	body weight
ER	endoplasmic reticulum
FA	fluorescein angiography
HPCD	2-hydroxypropyl-β-cyclodextrin

HPCD-FITC	6-deoxy-6-[(5/6)-fluoresceinylthioreido]-HPCD
LXR	liver X receptors
WT	wild type

REFERENCES

Abi-Mosleh L, Infante RE, Radhakrishnan A, Goldstein JL, & Brown MS (2009). Cyclodextrin overcomes deficient lysosome-to-endoplasmic reticulum transport of cholesterol in niemann-pick type c cells. Proc Natl Acad Sci U S A, 106(46), 19316–19321. 10.1073/pnas.0910916106 [PubMed: 19884502]

Actis Dato V, & Chiabrando GA (2018). The role of low-density lipoprotein receptor-related protein 1 in lipid metabolism, glucose homeostasis and inflammation. Int J Mol Sci, 19(6), 10.3390/ijms19061780

Alexander SPH, Fabbro D, Kelly E, Mathie A, Peters JA, Veale EL, et al. (2019). The concise guide to pharmacology 2019/20: Enzymes. British Journal of Pharmacology, 176(S1), S297–S396. 10.1111/bph.14752 [PubMed: 31710714]

Amar MJ, Kaler M, Courville AB, Shamburek R, Sampson M, & Remaley AT (2016). Randomized double blind clinical trial on the effect of oral alpha-cyclodextrin on serum lipids. Lipids Health Dis, 15(1), 115. 10.1186/s12944-016-0284-6 [PubMed: 27405337]

Atger VM, de la Llera Moya M, Stoudt GW, Rodrigueza WV, Phillips MC, & Rothblat GH (1997). Cyclodextrins as catalysts for the removal of cholesterol from macrophage foam cells. J Clin Invest, 99(4), 773–780. 10.1172/JCI119223 [PubMed: 9045882]

Bai M, Gad H, Turacchio G, Cocucci E, Yang JS, Li J, et al. (2011). Arfgap1 promotes ap-2-dependent endocytosis. Nat Cell Biol, 13(5), 559–567. 10.1038/ncb2221 [PubMed: 21499258]

Bok D, Galbraith G, Lopez I, Woodruff M, Nusinowitz S, BeltrandelRio H, et al. (2003). Blindness and auditory impairment caused by loss of the sodium bicarbonate cotransporter nbc3. Nat Genet, 34(3), 313–319. 10.1038/ng1176 [PubMed: 12808454]

Calias P (2017). 2-hydroxypropyl-beta-cyclodextrins and the blood-brain barrier: Considerations for niemann-pick disease type c1. Curr Pharm Des, 10.2174/1381612823666171019164220

Chen FW, Li C, & Ioannou YA (2010). Cyclodextrin induces calcium-dependent lysosomal exocytosis. PLoS One, 5(11), e15054. 10.1371/journal.pone.0015054 [PubMed: 21124786]

Christian AE, Haynes MP, Phillips MC, & Rothblat GH (1997). Use of cyclodextrins for manipulating cellular cholesterol content. J Lipid Res, 38(11), 2264–2272. [PubMed: 9392424]

Clayton EL, & Cousin MA (2009). The molecular physiology of activity-dependent bulk endocytosis of synaptic vesicles. J Neurochem, 111(4), 901–914. 10.1111/j.1471-4159.2009.06384.x [PubMed: 19765184]

Coisne C, Tilloy S, Monflier E, Wils D, Fenart L, & Gosselet F (2016). Cyclodextrins as emerging therapeutic tools in the treatment of cholesterol-associated vascular and neurodegenerative diseases. Molecules, 21(12), 10.3390/molecules21121748

Curcio CA, Millican CL, Bailey T, & Kruth HS (2001). Accumulation of cholesterol with age in human bruch's membrane. Invest Ophthalmol Vis Sci, 42(1), 265–274. [PubMed: 11133878]

Curcio CA, Presley JB, Malek G, Medeiros NE, Avery DV, & Kruth HS (2005). Esterified and unesterified cholesterol in drusen and basal deposits of eyes with age-related maculopathy. Exp Eye Res, 81(6), 731–741. 10.1016/j.exer.2005.04.012 [PubMed: 16005869]

Curtis MJ, Alexander S, Cirino G, Docherty JR, George CH, Giembycz MA, et al. (2018). Experimental design and analysis and their reporting ii: Updated and simplified guidance for authors and peer reviewers. Br J Pharmacol, 175(7), 987–993. 10.1111/bph.14153 [PubMed: 29520785]

Ding Y, Wu Y, Zeng R, & Liao K (2012). Proteomic profiling of lipid droplet-associated proteins in primary adipocytes of normal and obese mouse. Acta Biochim Biophys Sin (Shanghai), 44(5), 394–406. 10.1093/abbs/gms008 [PubMed: 22343379]

Gallegos AM, Atshaves BP, Storey SM, McIntosh AL, Petrescu AD, & Schroeder F (2001). Sterol carrier protein-2 expression alters plasma membrane lipid distribution and cholesterol dynamics. Biochemistry, 40(21), 6493–6506. [PubMed: 11371213]

Gannon J, Fernandez-Rodriguez J, Alamri H, Feng SB, Kalantari F, Negi S, et al. (2014). Arfgap1 is dynamically associated with lipid droplets in hepatocytes. PLoS One, 9(11), e111309. 10.1371/journal.pone.0111309 [PubMed: 25397679]

Gould S, & Scott RC (2005). 2-hydroxypropyl-beta-cyclodextrin (hp-beta-cd): A toxicology review. Food Chem Toxicol, 43(10), 1451–1459. 10.1016/j.fct.2005.03.007 [PubMed: 16018907]

Guymer RH, Baird PN, Varsamidis M, Busija L, Dimitrov PN, Aung KZ, et al. (2013). Proof of concept, randomized, placebo-controlled study of the effect of simvastatin on the course of age-related macular degeneration. PLoS One, 8(12), e83759. 10.1371/journal.pone.0083759 [PubMed: 24391822]

Hara T, Inami M, & Hara T (1998). Efficacy and safety of fluorescein angiography with orally administered sodium fluorescein. Am J Ophthalmol, 126(4), 560–564. 10.1016/s0002-9394(98)00112-3 [PubMed: 9780101]

Harding SD, Sharman JL, Faccenda E, Southan C, Pawson AJ, Ireland S, et al. (2017). The iuphar/bps guide to pharmacology in 2018: Updates and expansion to encompass the new guide to immunopharmacology. Nucleic Acids Research, 46(D1), D1091–D1106. 10.1093/nar/gkx1121

Harju AK, Bootorabi F, Kuuslahti M, Supuran CT, & Parkkila S (2013). Carbonic anhydrase iii: A neglected isozyme is stepping into the limelight. J Enzyme Inhib Med Chem, 28(2), 231–239. 10.3109/14756366.2012.700640 [PubMed: 22803676]

Hattori Y, Ohta S, Hamada K, Yamada-Okabe H, Kanemura Y, Matsuzaki Y, et al. (2007). Identification of a neuron-specific human gene, kiaa1110, that is a guanine nucleotide exchange factor for arf1. Biochem Biophys Res Commun, 364(4), 737–742. 10.1016/j.bbrc.2007.10.041 [PubMed: 17981261]

Huang J, Weinfurter S, Pinto PC, Pretze M, Kranzlin B, Pill J, et al. (2016). Fluorescently labeled cyclodextrin derivatives as exogenous markers for real-time transcutaneous measurement of renal function. Bioconjug Chem, 27(10), 2513–2526. 10.1021/acs.bioconjchem.6b00452 [PubMed: 27611623]

Igarashi M, Osuga J, Isshiki M, Sekiya M, Okazaki H, Takase S, et al. (2010). Targeting of neutral cholesterol ester hydrolase to the endoplasmic reticulum via its n-terminal sequence. J Lipid Res, 51(2), 274–285. 10.1194/jlr.M900201-JLR200 [PubMed: 19592704]

Inglis-Broadgate SL, Ocaka L, Banerjee R, Gaasenbeek M, Chapple JP, Cheetham ME, et al. (2005). Isolation and characterization of murine cds (cdp-diacylglycerol synthase) 1 and 2. Gene, 356(19–31. 10.1016/j.gene.2005.04.037 [PubMed: 16023307]

Irie T, Fukunaga K, Garwood MK, Carpenter TO, Pitha J, & Pitha J (1992). Hydroxypropylcyclodextrins in parenteral use. Ii: Effects on transport and disposition of lipids in rabbit and humans. J Pharm Sci, 81(6), 524–528. [PubMed: 1522488]

Irie T, & Uekama K (1997). Pharmaceutical applications of cyclodextrins. Iii. Toxicological issues and safety evaluation. J Pharm Sci, 86(2), 147–162. 10.1021/js960213f [PubMed: 9040088]

Janowski BA, Grogan MJ, Jones SA, Wisely GB, Kliewer SA, Corey EJ, et al. (1999). Structural requirements of ligands for the oxysterol liver x receptors lxralpha and lxrbeta. Proc Natl Acad Sci U S A, 96(1), 266–271. [PubMed: 9874807]

Jerome-Majewska LA, Achkar T, Luo L, Lupu F, & Lacy E (2010). The trafficking protein tmed2/p24beta(1) is required for morphogenesis of the mouse embryo and placenta. Developmental biology, 341(1), 154–166. 10.1016/j.ydbio.2010.02.019 [PubMed: 20178780]

Kadurin I, Rothwell SW, Lana B, Nieto-Rostro M, & Dolphin AC (2017). Lrp1 influences trafficking of n-type calcium channels via interaction with the auxiliary alpha2delta-1 subunit. Sci Rep, 7(43802. 10.1038/srep43802 [PubMed: 28256585]

Kam JH, Lynch A, Begum R, Cunea A, & Jeffery G (2015). Topical cyclodextrin reduces amyloid beta and inflammation improving retinal function in ageing mice. Exp Eye Res, 135(59–66. 10.1016/j.exer.2015.03.023 [PubMed: 25921262]

Kawabe H, Sakisaka T, Yasumi M, Shingai T, Izumi G, Nagano F, et al. (2003). A novel rabconnectin-3-binding protein that directly binds a gdp/gtp exchange protein for rab3a small

g protein implicated in ca(2+)-dependent exocytosis of neurotransmitter. Genes Cells, 8(6), 537–546. 10.1046/j.1365-2443.2003.00655.x [PubMed: 12786944]

Kilka S, Erdmann F, Migdoll A, Fischer G, & Weiwad M (2009). The proline-rich n-terminal sequence of calcineurin abeta determines substrate binding. Biochemistry, 48(9), 1900–1910. 10.1021/bi8019355 [PubMed: 19154138]

Kraemer R, Pomerantz KB, Kesav S, Scallen TJ, & Hajjar DP (1995). Cholesterol enrichment enhances expression of sterol-carrier protein-2: Implications for its function in intracellular cholesterol trafficking. J Lipid Res, 36(12), 2630–2638. [PubMed: 8847489]

Li F, & Zhang H (2019). Lysosomal acid lipase in lipid metabolism and beyond. Arterioscler Thromb Vasc Biol, 39(5), 850–856. 10.1161/atvbaha.119.312136 [PubMed: 30866656]

Liu B, Ramirez CM, Miller AM, Repa JJ, Turley SD, & Dietschy JM (2010). Cyclodextrin overcomes the transport defect in nearly every organ of npc1 mice leading to excretion of sequestered cholesterol as bile acid. J Lipid Res, 51(5), 933–944. 10.1194/jlr.M000257 [PubMed: 19965601]

Liu B, Turley SD, Burns DK, Miller AM, Repa JJ, & Dietschy JM (2009). Reversal of defective lysosomal transport in npc disease ameliorates liver dysfunction and neurodegeneration in the npc1−/− mouse. Proc Natl Acad Sci U S A, 106(7), 2377–2382. 10.1073/pnas.0810895106 [PubMed: 19171898]

Mast N, Reem R, Bederman I, Huang S, DiPatre PL, Björkhem I, et al. (2011). Cholestenoic acid is an important elimination product of cholesterol in the retina: Comparison of retinal cholesterol metabolism with that in the brain. Invest Ophthalmol Vis Sci, 52(1), 594–603. 10.1167/iovs.10-6021 [PubMed: 20881306]

Mast N, Shafaati M, Zaman W, Zheng W, Prusak D, Wood T, et al. (2010). Marked variability in hepatic expression of cytochromes cyp7a1 and cyp27a1 as compared to cerebral cyp46a1. Lessons from a dietary study with omega 3 fatty acids in hamsters. Biochim Biophys Acta, 1801(6), 674–681. 10.1016/j.bbalip.2010.03.005 [PubMed: 20298807]

Merkulova M, Paunescu TG, Azroyan A, Marshansky V, Breton S, & Brown D (2015). Mapping the h(+) (v)-atpase interactome: Identification of proteins involved in trafficking, folding, assembly and phosphorylation. Sci Rep, 5(14827. 10.1038/srep14827 [PubMed: 26442671]

Miller JW (2013). Age-related macular degeneration revisited--piecing the puzzle: The lxix edward jackson memorial lecture. Am J Ophthalmol, 155(1), 1–35 e13. 10.1016/j.ajo.2012.10.018 [PubMed: 23245386]

Nagano F, Kawabe H, Nakanishi H, Shinohara M, Deguchi-Tawarada M, Takeuchi M, et al. (2002). Rabconnectin-3, a novel protein that binds both gdp/gtp exchange protein and gtpase-activating protein for rab3 small g protein family. J Biol Chem, 277(12), 9629–9632. 10.1074/jbc.C100730200 [PubMed: 11809763]

Nociari MM, Lehmann GL, Perez Bay AE, Radu RA, Jiang Z, Goicochea S, et al. (2014). Beta cyclodextrins bind, stabilize, and remove lipofuscin bisretinoids from retinal pigment epithelium. Proc Natl Acad Sci U S A, 111(14), E1402–1408. 10.1073/pnas.1400530111 [PubMed: 24706818]

Oak ASW, Messinger JD, & Curcio CA (2014). Subretinal drusenoid deposits: Further characterization by lipid histochemistry. Retina, 34(4), 825–826. Doi 10.1097/Iae.0000000000000121 [PubMed: 24589874]

Ohtani Y, Irie T, Uekama K, Fukunaga K, & Pitha J (1989). Differential effects of alpha-, beta- and gamma-cyclodextrins on human erythrocytes. Eur J Biochem, 186(1–2), 17–22. [PubMed: 2598927]

Okazaki H, Igarashi M, Nishi M, Sekiya M, Tajima M, Takase S, et al. (2008). Identification of neutral cholesterol ester hydrolase, a key enzyme removing cholesterol from macrophages. J Biol Chem, 283(48), 33357–33364. 10.1074/jbc.M802686200 [PubMed: 18782767]

Petrov AM, Astafev AA, Mast N, Saadane A, El-Darzi N, & Pikuleva IA (2019). The interplay between retinal pathways of cholesterol output and its effects on mouse retina. Biomolecules, 9(12), 10.3390/biom9120867

Pfaffl MW (2001). A new mathematical model for relative quantification in real-time rt-pcr. Nucleic Acids Res, 29(9), e45. [PubMed: 11328886]

Pfrieger FW, & Ungerer N (2011). Cholesterol metabolism in neurons and astrocytes. Prog Lipid Res, 50(4), 357–371. 10.1016/j.plipres.2011.06.002 [PubMed: 21741992]

Pitha J, Irie T, Sklar PB, & Nye JS (1988). Drug solubilizers to aid pharmacologists: Amorphous cyclodextrin derivatives. Life Sci, 43(6), 493–502. [PubMed: 2841549]

Plazzo AP, Hofer CT, Jicsinszky L, Fenyvesi E, Szente L, Schiller J, et al. (2012). Uptake of a fluorescent methyl-beta-cyclodextrin via clathrin-dependent endocytosis. Chem Phys Lipids, 165(5), 505–511. 10.1016/j.chemphyslip.2012.03.007 [PubMed: 22503802]

Pu J, Guardia CM, Keren-Kaplan T, & Bonifacino JS (2016). Mechanisms and functions of lysosome positioning. J Cell Sci, 129(23), 4329–4339. 10.1242/jcs.196287 [PubMed: 27799357]

Qi Y, Kapterian TS, Du X, Ma Q, Fei W, Zhang Y, et al. (2016). Cdp-diacylglycerol synthases regulate the growth of lipid droplets and adipocyte development. J Lipid Res, 57(5), 767–780. 10.1194/jlr.M060574 [PubMed: 26946540]

Reti-Nagy K, Malanga M, Fenyvesi E, Szente L, Vamosi G, Varadi J, et al. (2015). Endocytosis of fluorescent cyclodextrins by intestinal caco-2 cells and its role in paclitaxel drug delivery. Int J Pharm, 496(2), 509–517. 10.1016/j.ijpharm.2015.10.049 [PubMed: 26498369]

Rosenbaum AI, Zhang G, Warren JD, & Maxfield FR (2010). Endocytosis of beta-cyclodextrins is responsible for cholesterol reduction in niemann-pick type c mutant cells. Proc Natl Acad Sci U S A, 107(12), 5477–5482. 10.1073/pnas.0914309107 [PubMed: 20212119]

Saadane A, Mast N, Charvet C, Omarova S, Zheng W, Huang SS, et al. (2014a). Retinal and non-ocular abnormalities in cyp27a1−/− cyp64a1−/− mice with dysfunctional metabolism of cholesterol. Amer J Pathol, 184(9), 2403–2419. [PubMed: 25065682]

Saadane A, Mast N, Charvet CD, Omarova S, Zheng W, Huang SS, et al. (2014b). Retinal and nonocular abnormalities in cyp27a1(−/−)cyp46a1(−/−) mice with dysfunctional metabolism of cholesterol. Am J Pathol, 184(9), 2403–2419. 10.1016/j.ajpath.2014.05.024 [PubMed: 25065682]

Saadane A, Mast N, Dao T, Ahmad B, & Pikuleva IA (2016). Retinal hypercholesterolemia triggers cholesterol accumulation and esterification in photoreceptor cells. J Biol Chem, 291(39), 20427–20439. 10.1074/jbc.M116.744656 [PubMed: 27514747]

Saadane A, Mast N, Trichonas G, Chakraborty D, Hammer S, Busik JV, et al. (2019). Retinal vascular abnormalities and microglia activation in mice with deficiency in cytochrome p450 46a1-mediated cholesterol removal. Am J Pathol, 189(2), 405–425. 10.1016/j.ajpath.2018.10.013 [PubMed: 30448403]

Saadane A, Petrov A, Mast N, El-Darzi N, Dao T, Alnemri A, et al. (2018). Mechanisms that minimize retinal impact of apolipoprotein e absence. J Lipid Res, 59(12), 2368–2382. 10.1194/jlr.M090043 [PubMed: 30333155]

Schroeder F, Atshaves BP, McIntosh AL, Gallegos AM, Storey SM, Parr RD, et al. (2007). Sterol carrier protein-2: New roles in regulating lipid rafts and signaling. Biochim Biophys Acta, 1771(6), 700–718. 10.1016/j.bbalip.2007.04.005 [PubMed: 17543577]

Sedlyarov V, Eichner R, Girardi E, Essletzbichler P, Goldmann U, Nunes-Hasler P, et al. (2018). The bicarbonate transporter slc4a7 plays a key role in macrophage phagosome acidification. Cell Host Microbe, 23(6), 766–774 e765. 10.1016/j.chom.2018.04.013 [PubMed: 29779931]

Shiba Y, Luo R, Hinshaw JE, Szul T, Hayashi R, Sztul E, et al. (2011). Arfgap1 promotes copi vesicle formation by facilitating coatomer polymerization. Cell Logist, 1(4), 139–154. 10.4161/cl.1.4.18896 [PubMed: 22279613]

Spann NJ, Garmire LX, McDonald JG, Myers DS, Milne SB, Shibata N, et al. (2012). Regulated accumulation of desmosterol integrates macrophage lipid metabolism and inflammatory responses. Cell, 151(1), 138–152. 10.1016/j.cell.2012.06.054 [PubMed: 23021221]

Squirrell D, Dinakaran S, Dhingra S, Mody C, Brand C, & Talbot J (2005). Oral fluorescein angiography with the scanning laser ophthalmoscope in diabetic retinopathy: A case controlled comparison with intravenous fluorescein angiography. Eye (Lond), 19(4), 411–417. 10.1038/sj.eye.6701513 [PubMed: 15184968]

Tachikui H, Navet AF, & Ozawa M (1997). Identification of the ca(2+)-binding domains in reticulocalbin, an endoplasmic reticulum resident ca(2+)-binding protein with multiple ef-hand motifs. J Biochem, 121(1), 145–149. [PubMed: 9058205]

Takada N, Naito T, Inoue T, Nakayama K, Takatsu H, & Shin HW (2018). Phospholipid-flipping activity of p4-atpase drives membrane curvature. EMBO J, 37(9), 10.15252/embj.201797705

Theofilopoulos S, Griffiths WJ, Crick PJ, Yang S, Meljon A, Ogundare M, et al. (2014). Cholestenoic acids regulate motor neuron survival via liver x receptors. J Clin Invest, 124(11), 4829–4842. 10.1172/JCI68506 [PubMed: 25271621]

Turner PV, Brabb T, Pekow C, & Vasbinder MA (2011). Administration of substances to laboratory animals: Routes of administration and factors to consider. Journal of the American Association for Laboratory Animal Science : JAALAS, 50(5), 600–613. [PubMed: 22330705]

Uekama K, Hirayama F, & Irie T (1998). Cyclodextrin drug carrier systems. Chem Rev, 98(5), 2045–2076. [PubMed: 11848959]

Valapala M, Sergeev Y, Wawrousek E, Hose S, Zigler JS Jr., & Sinha D (2016). Modulation of v-atpase by betaa3/a1-crystallin in retinal pigment epithelial cells. Adv Exp Med Biol, 854(779–784. 10.1007/978-3-319-17121-0_104 [PubMed: 26427489]

Vavvas DG, Daniels AB, Kapsala ZG, Goldfarb JW, Ganotakis E, Loewenstein JI, et al. (2016). Regression of some high-risk features of age-related macular degeneration (amd) in patients receiving intensive statin treatment. EBioMedicine, 5(198–203. 10.1016/j.ebiom.2016.01.033 [PubMed: 27077128]

Watson AP, & Rosen ES (1990). Oral fluorescein angiography: Reassessment of its relative safety and evaluation of optimum conditions with use of capsules. Br J Ophthalmol, 74(8), 458–461. 10.1136/bjo.74.8.458 [PubMed: 2390518]

Wong WL, Su X, Li X, Cheung CM, Klein R, Cheng CY, et al. (2014). Global prevalence of age-related macular degeneration and disease burden projection for 2020 and 2040: A systematic review and meta-analysis. Lancet Glob Health, 2(2), e106–116. 10.1016/S2214-109X(13)70145-1 [PubMed: 25104651]

Wozniak MJ, & Allan VJ (2006). Cargo selection by specific kinesin light chain 1 isoforms. EMBO J, 25(23), 5457–5468. 10.1038/sj.emboj.7601427 [PubMed: 17093494]

Wu T, Tian J, Cutler RG, Telljohann RS, Bernlohr DA, Mattson MP, et al. (2010). Knockdown of fabp5 mrna decreases cellular cholesterol levels and results in decreased apob100 secretion and triglyceride accumulation in arpe-19 cells. Lab Invest, 90(6), 906–914. 10.1038/labinvest.2009.33 [PubMed: 19434059]

Yeaman SJ (2004). Hormone-sensitive lipase--new roles for an old enzyme. Biochem J, 379(Pt 1), 11–22. 10.1042/BJ20031811 [PubMed: 14725507]

Zimmer S, Grebe A, Bakke SS, Bode N, Halvorsen B, Ulas T, et al. (2016). Cyclodextrin promotes atherosclerosis regression via macrophage reprogramming. Sci Transl Med, 8(333), 333ra350. 10.1126/scitranslmed.aad6100

BULLET POINT SUMMARY:

What is already known:

- HPCD lowers tissue cholesterol *in vitro* and *in vivo*.
- HPCD does not cross the blood-brain barrier and has unknown permeability of the blood-retina barrier.

What this study adds:

- HPCD can enter the retina and alter the retinal sterol, gene, and protein levels.
- Similar mechanisms but different proteins mediate retinal HPCD effects in wild type and *Cyp27a1*$^{-/-}$*Cyp46a1*$^{-/-}$ mice.

Clinical significance:

- HPCD should further be evaluated as a potential therapeutic for age-related macular degeneration.

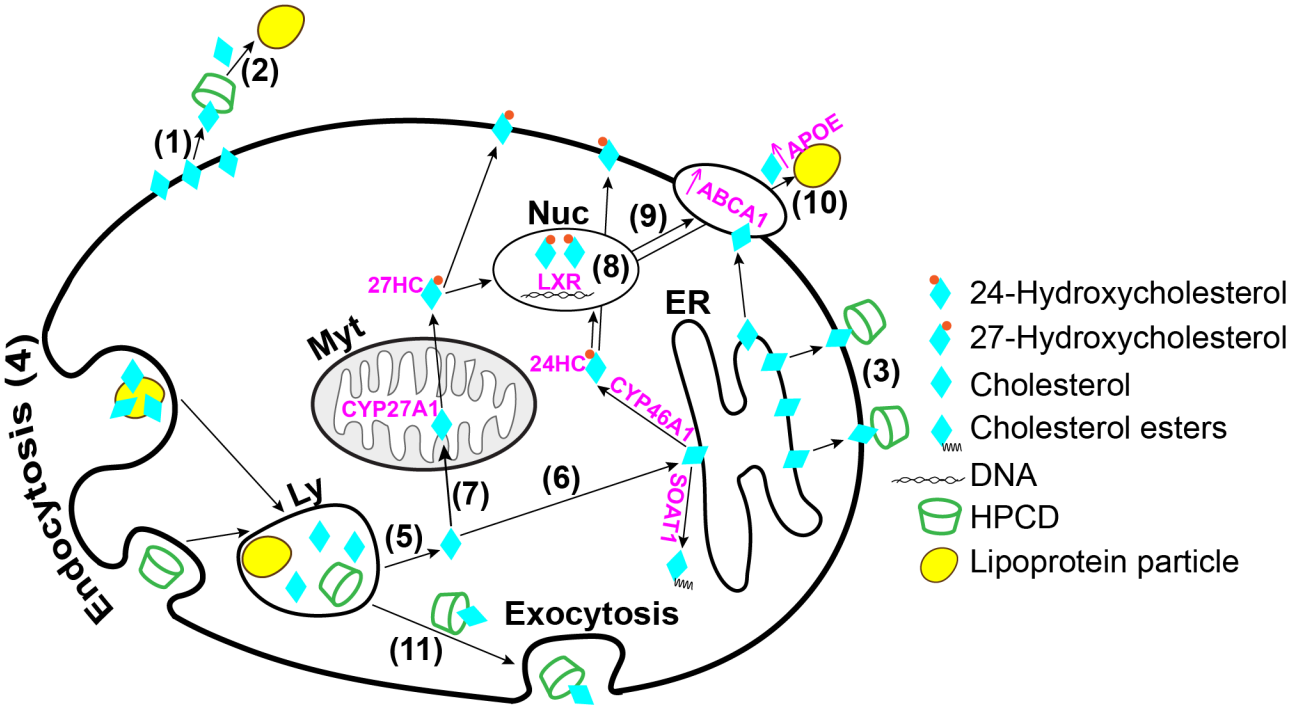

Figure 1.

Schematic summary of the mechanisms whereby HPCD can lower cellular cholesterol. HPCD can extract cholesterol from the plasma membranes (1) and either function as a cholesterol shuttle to the apolipoproteins (2) in the systemic circulation (Atger et al., 1997) or retain cholesterol (3) while in the systemic circulation. HPCD can also enter cells, the late endosomal/lysosomal compartment (4), *via* endo/pinocytosis (Plazzo et al., 2012; Rosenbaum et al., 2010) and then release the lysosomal cholesterol into the cytoplasm (5) for subsequent cellular processing (Abi-Mosleh et al., 2009; Liu et al., 2010; Liu et al., 2009). This processing can include cholesterol flow from the lysosomes to the endoplasmic reticulum (6) for esterification by SOAT1 or hydroxylation by CYP7A1 in the liver and CYP46A1 in the CNS as well as transport to the mitochondria (7) for hydroxylation by CYP11A1 in the brain and steroidogenic tissues and CYP27A1 in many extrahepatic tissues. 24- and 27-Hydroxycholesterols produced by CYP46A1 and CYP27A1, respectively, can activate LXRs (Janowski et al., 1999), transcription factors controlling the expression of genes from different metabolic pathways. Hence, HPCD can activate the LXR signaling (8) by increasing the 24- and 27-hydroxycholesterol production and thereby cellular cholesterol efflux *via* the LXR-target genes ABCA1 (9) and APOE (10) (Zimmer et al., 2016). Finally, HPCD may reduce cellular cholesterol through stimulation of lysosomal exocytosis (11) (Chen et al., 2010). Ly, lysosome; Myt, mitochondrion; Nuc, nucleus, ER, endoplasmic reticulum.

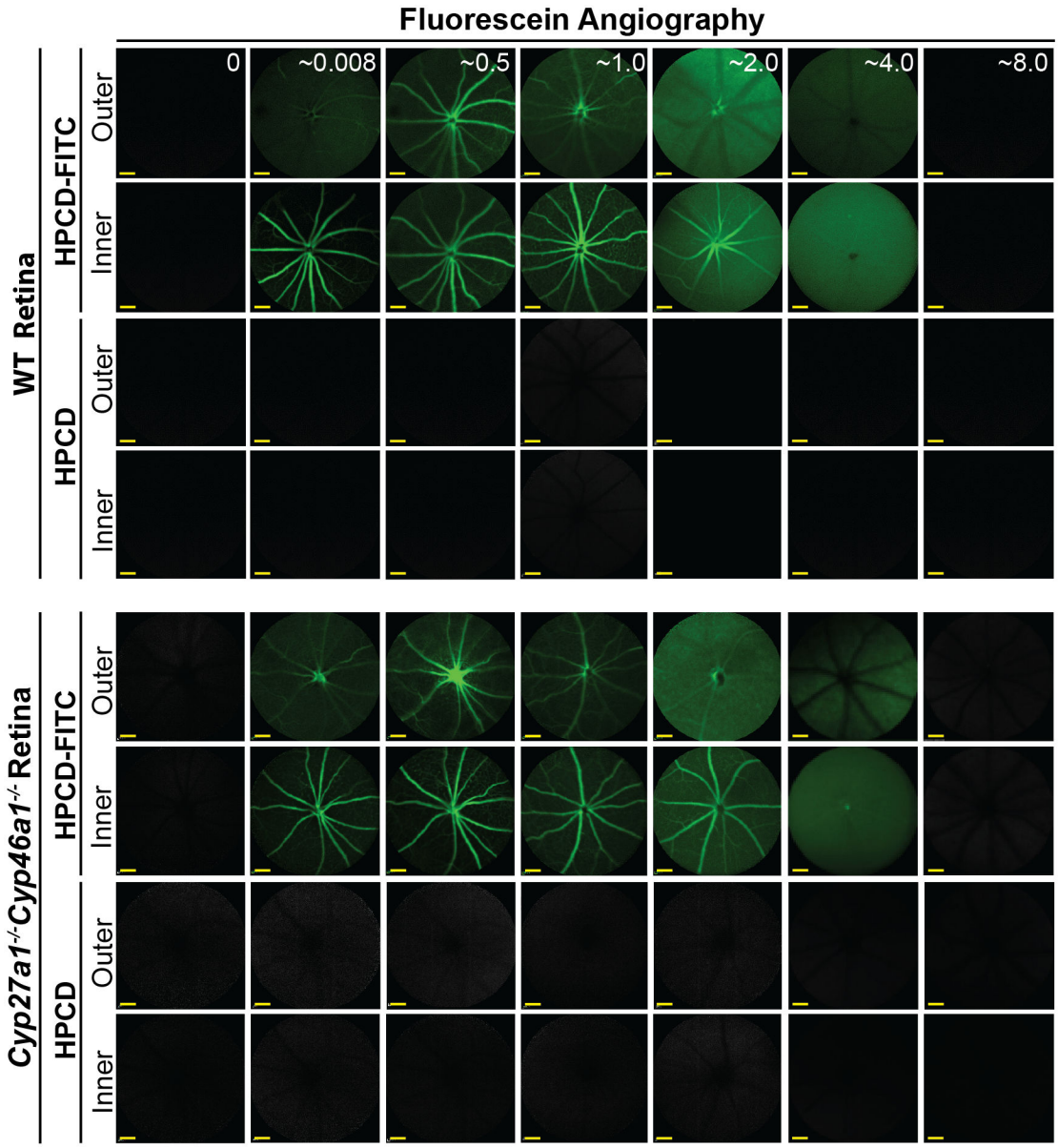

Figure 2.

Fluorescein angiography (55° field of view) of mice injected i.p. either with HPCD or HPCD-FITC. The laser beam was first focused on the outer and then inner retina to assess the two distinct vascular networks, the choroidal and intraretinal, which nourish the outer and inner retina, respectively. Five female mice were used to collect the data for the 0–0.5-, 1-, 2-, 4-, and 8-hr post-injection time points; the post injection time (hr) is in white font on the upper panels. Scale bars: 100 μm.

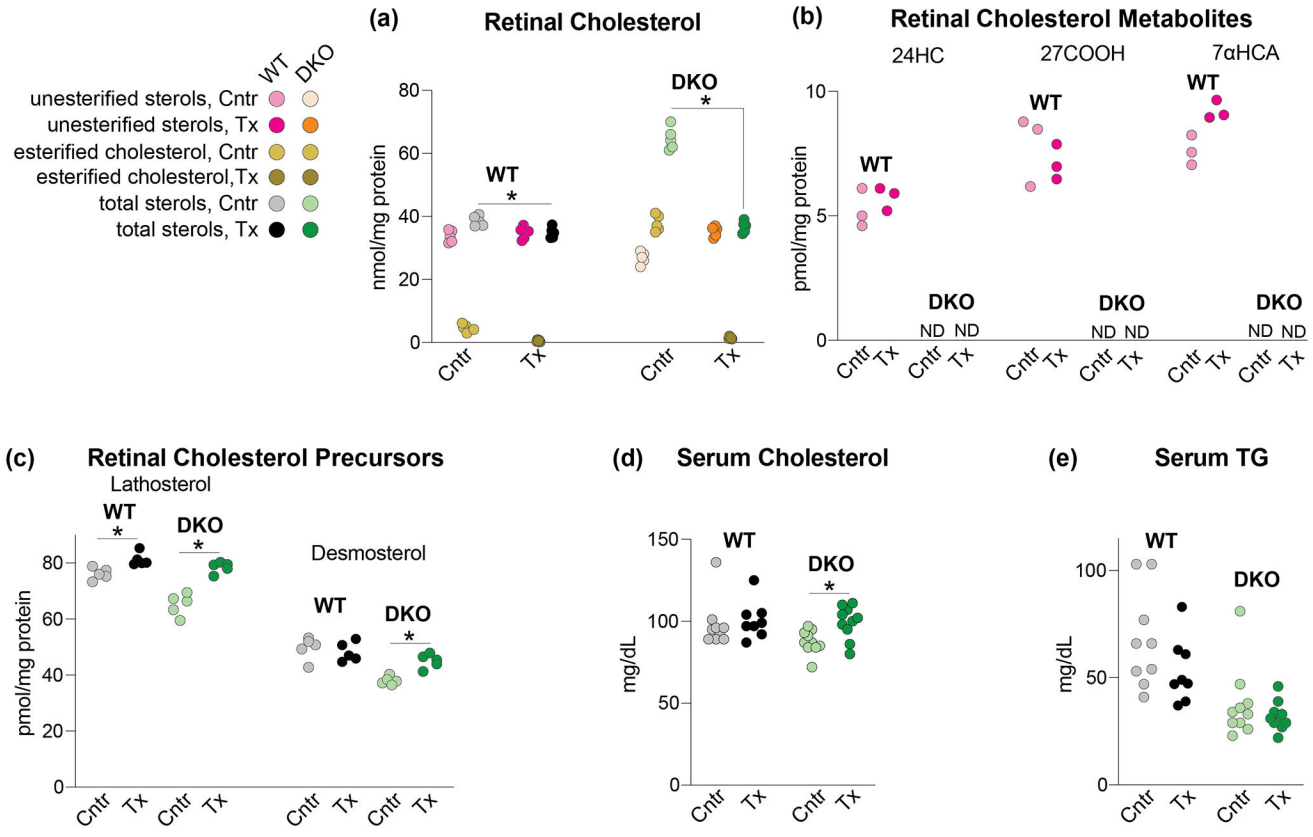

Figure 3.

HPCD treatment by oral gavage: effects on lipids. The HPCD dose was 1.6 g/kg BW and treatment duration was 11 days. (a-c) Sterols in the retina. The total sterol content is a sum of the esterified and unesterified sterol forms. (d, e) Lipids in the serum. (a) and (c-e) Each dot represents an individual measurement of a male retina; 5 mice in each group in (a) and (c) and 8–10 mice in each group in (d) and (e) were used. (b) Each dot represents a measurement of a pooled sample of 6 retinas from 6 male mice; a total of three pooled samples (18 mice) were used for each group. Statistical significance for changes in total sterol in HPCD-treated *vs* control mice in (a) and (c-e), was assessed by the Mann-Whitney *U* test and that in (b) was not assessed because of n=3. $*P \leq 0.05$. 24HC, 24-hydroxycholesterol; 27COOH, 5-cholestenoic acid; 7αHCA, 7α-hydroxy-3-oxo-4-cholestenoic acid; Cntr, control mice; DKO, *Cyp27a1*$^{-/-}$*Cyp46a1*$^{-/-}$ mice; ND, not detected; TG, triglycerides; Tx, HPCD-treated mice; WT, wild type mice;

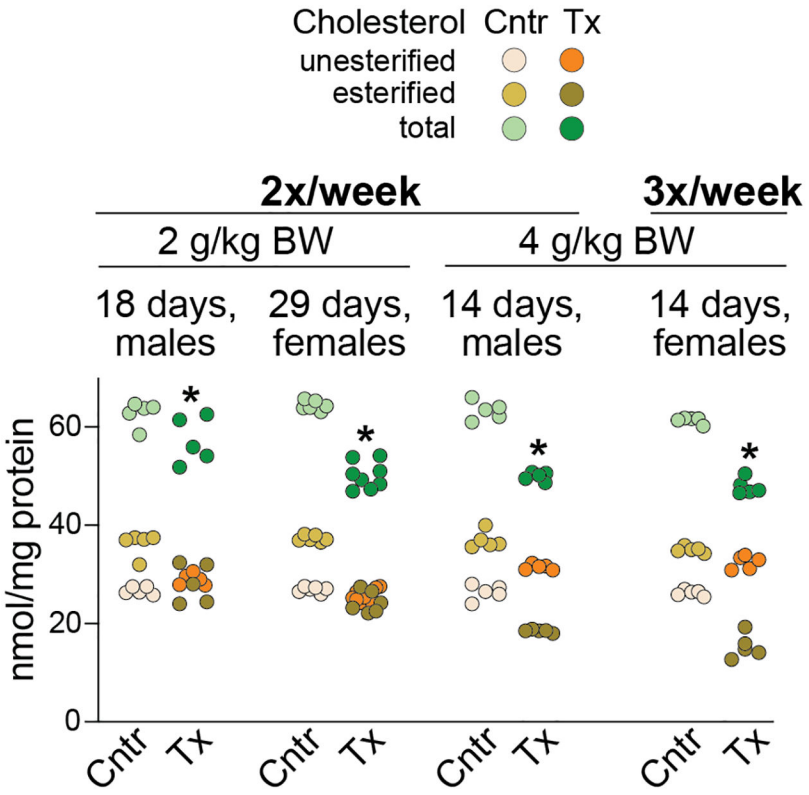

Figure 4.

HPCD treatment by subcutaneous injections: effects on retinal cholesterol of *Cyp27a1*$^{-/-}$*Cyp46a1*$^{-/-}$ mice. Dots represent individual measurements in mouse retina (5–8 mice per group). The total cholesterol content is a sum of the esterified and unesterified cholesterol. Statistical significance for changes in total cholesterol in HPCD-treated *vs* control mice was assessed by the Mann-Whitney *U* test. *$P \leq 0.05$. 2x, 2 injections; 3x, three injections; Cntrl, control mice; BW, body weight; Tx, HPCD-treated mice.

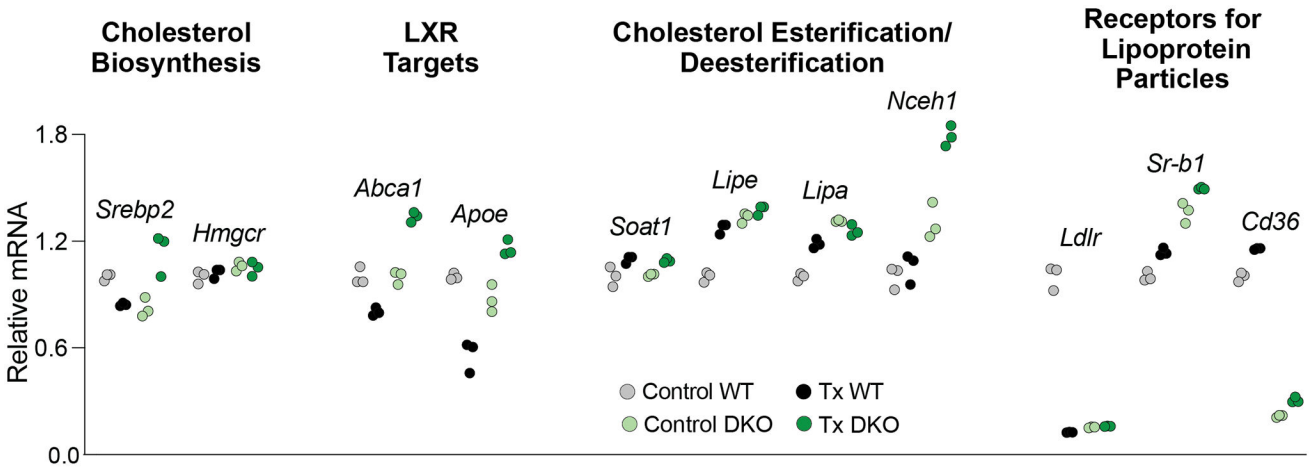

Figure 5.

HPCD treatment by oral gavage: effects on retinal gene expression. The treatment paradigm was the same as in Figure 3. Changes in the relative mRNA levels were normalized to the gene expression in control WT mice. *Srebp2* encodes a transcription factor, which senses the intracellular cholesterol levels and modulates the expression of many genes involved in the pathway of cholesterol biosynthesis. *Hmgcr* is one of SREBP2 targets and is the rate limiting enzyme of this pathway. *Abca1* encodes a transporter, which effluxes cholesterol excess out of cells. *Apoe* encodes an apolipoprotein and a constituent of apolipoprotein particles, which accept cholesterol excess effluxed by ABCA1. *Soat1* encodes a ubiquitous cholesterol esterifying enzyme, whereas *Lipe*, *Lipa*, and *Nceh1* are the genes for three different cholesterol ester hydrolyzing enzymes. *Ldlr*, *Sr-b1*, and *Cd36* encode the plasma receptors for different lipoprotein particles. Dots represent triplicate measurements on one pooled sample of 8 retinas from 8 male mice. Statistical significance was not assessed as n=1. Instead, an arbitrary cut off was used, which was ≥32% change in gene expression between control WT *vs* control *Cyp27a1*$^{-/-}$*Cyp46a1*$^{-/-}$ mice or between HPCD-treated *vs* control mice of the same genotype. This cut off represented two times 16%, the highest SD value in our triplicate technical replicates. Cntr, control mice; DKO, *Cyp27a1*$^{-/-}$*Cyp46a1*$^{-/-}$ mice; Tx, HPCD-treated mice; WT, wild type mice.

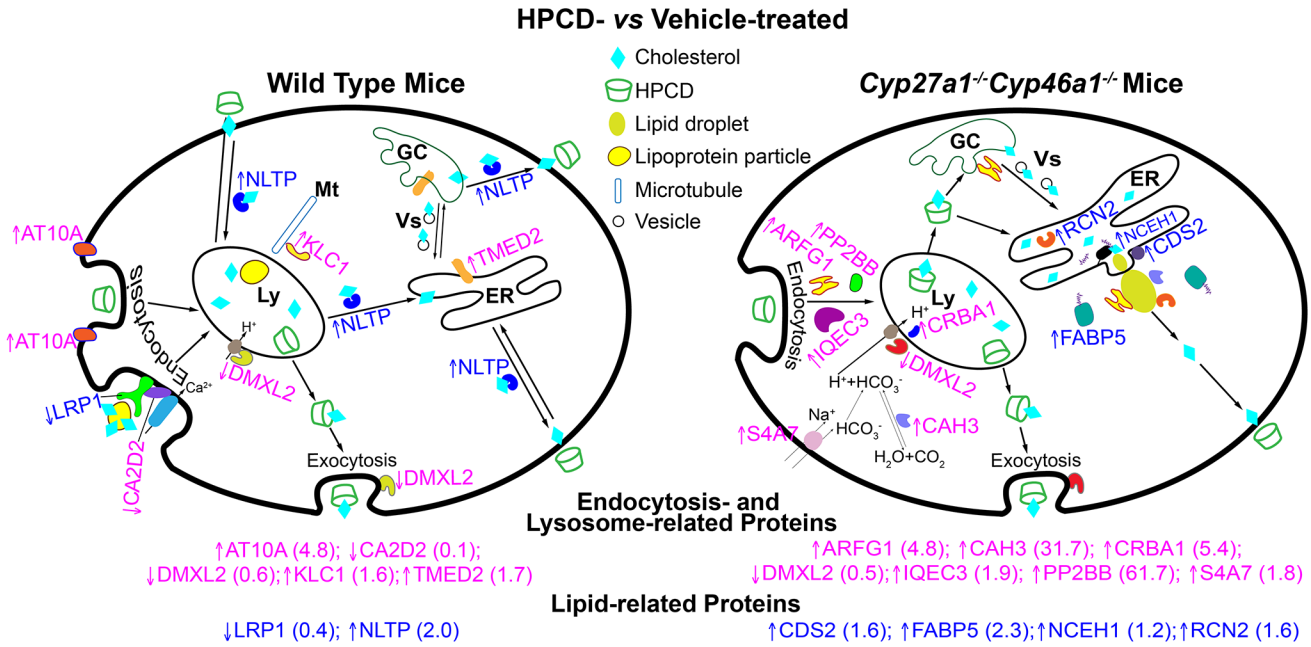

Figure 6.

HPCD treatment by oral gavage: effects on retinal proteomics. The treatment paradigm was the same as in Figure 3. Upwards and downwards arrows indicate increased and decreased protein abundance, respectively; a fold-change in abundance is shown in parenthesis. The affected proteins in the WT retina include AT10A, the catalytic component of a P4-ATPase flippase complex, which promotes inward bending of the plasma membranes and hence endocytosis (Takada et al., 2018). LRP1 is the low density lipoprotein receptor-related protein 1, which binds and internalizes lipoproteins particles containing cholesterol (Actis Dato & Chiabrando, 2018). LRP1 interacts with CA2D2, the $\alpha_2\delta$ subunit of the voltage-dependent calcium channels, and through this interaction affects the channel function and trafficking (Kadurin et al., 2017). DMXL2 is the α subunit of rabconnectin-3, a multifunction protein, which is involved in the regulation of Ca^{2+}-dependent exocytosis (Kawabe et al., 2003; Nagano et al., 2002). In addition, DMXL2 is required for the V-ATPase-driven lysosomal (Ly) acidification (Merkulova et al., 2015). KLC1 is a light chain of kinesin-1, a microtubule (Mt) motor protein involved in the movement of multiple cytoplasmic organelles, including lysosomes (Pu et al., 2016; Wozniak & Allan, 2006). TMED2 is a transmembrane emp24 domain-containing protein 2 involved in vesicular (Vs) trafficking between the endoplasmic reticulum (ER) and Golgi complex (GC) (Jerome-Majewska et al., 2010). NLTP is a sterol carrier protein-2 important for the intracellular cholesterol and other lipid trafficking (Gallegos et al., 2001; Kraemer et al., 1995; Schroeder et al., 2007). The affected proteins in the *Cyp27a1*$^{-/-}$*Cyp46a1*$^{-/-}$ retina include ARFG1, a multifunctional GTPase-activating protein for ADP-ribosylation factor 1 (ARF1), which participates in the adaptor protein 2-regulated endocytosis, vesicular biogenesis in the GC (a component of the coat protein I complex), and lipid droplet (LD) formation by transiently associating with LDs (Bai et al., 2011; Gannon et al., 2014; Shiba et al., 2011). IQEC3 is another protein pertinent to ARF1 as IQEC3 is a guanine nucleotide exchange factor for ARF1 (Hattori et al., 2007). PP2BB is a catalytic subunit of the

Ca^{2+}-dependent, calmodulin-stimulated phosphatase 2B (calcineurin), a multifunctional enzyme whose activity is required for synaptic vesicle endocytosis (Clayton & Cousin, 2009; Kilka et al., 2009). CRBA1 is a βA3/A1-crystallin, localized in the lysosomes of the retinal pigment epithelium where it regulates endolysosomal acidification by maintaining the activity of the lysosomal V-ATPase complex (Valapala et al., 2016). The V-ATPase-driven lysosomal acidification also requires DMXL2 (see above) (Merkulova et al., 2015). S4A7 is an electroneutral sodium bicarbonate cotransporter 3, which regulates intracellular pH and is essential for phagosome acidification (Bok et al., 2003; Sedlyarov et al., 2018). Intracellular pH is also affected by the activity of CAH3, the carbonic anhydrase 3 that catalyzes reversible hydration of carbon dioxide (Harju et al., 2013). CAH3 was also found on the surface of LDs as is RCN2, a Ca^{2+}-binding, mostly a luminal protein of the endoplasmic reticulum (Ding et al., 2012; Tachikui et al., 1997). CDS2 is a phosphatidic acid cytidylyltransferase 2 and an ER enzyme important for phospholipid metabolism (Inglis-Broadgate et al., 2005). CDS2 was also found to negatively regulate the growth of LDs (Qi et al., 2016). FABP5 is a cytoplasmic fatty acid-binding protein involved in intracellular transport of free fatty acids and thereby cholesterol and triglyceride metabolism (Wu et al., 2010). Finally, NCEH1 is a neutral cholesterol ester hydrolase (also known as KIAA1363 or arylacetamide deacetylase-like 1) tethered to the ER membrane by its N-terminus with its catalytic domain residing in the ER lumen (Igarashi et al., 2010; Okazaki et al., 2008).

Table 1.

Retinal proteins with differential abundance (≥1.5-fold) in the HPCD-treated (Tx) *vs* control (Cntr) WT mice. Protein grouping is by process and shows each protein only in one group despite the involvement in multiple processes. Proteins with a decreased expression are in bold.

Protein	№ of Peptides with Significant Changes in Abundance	№ of Unique Peptides	Sequence Coverage (%)	Peptide Intensity (a.u.) × 10^6		Tx/Cntr, Protein Ratio
				Tx	Cntr	
Vesicular Transport and Cytoskeletal Organization						
AT10A	2	2	1	0.29 ± 0.03	0.06 ± 0.01	4.8
CA2D2	**2**	**2**	**3**	**0.02 ± 0.04**	**0.28 ± 0.09**	**0.1**
DMXL2	**20**	**17**	**13**	**0.60 ± 0.1**	**0.96 ± 0.06**	**0.6**
K2C1	8	3	7	2.98 ± 0.75	1.73 ± 0.23	1.7
KLC1	2	2	5	0.27 ± 0.02	0.17 ± 0.05	1.6
LRP1	**2**	**2**	**1**	**0.17 ± 0.06**	**0.39 ± 0.03**	**0.4**
LZTL1	**3**	**3**	**14**	**0.25 ± 0.08**	**0.43± 0.04**	**0.6**
M4K2	3	2	2	1.56 ± 0.07	0.60 ± 0.28	2.6
OPTN	**3**	**3**	**7**	**0.18 ± 0.01**	**0.32 ± 0.07**	**0.5**
TMED2	2	2	7	0.37 ± 0.02	0.21 ± 0.09	1.7
TPPP3	**4**	**4**	**22**	**0.49 ± 0.16**	**0.78 ± 0.05**	**0.6**
Metabolism and Energy Homeostasis						
AL3A1	**7**	**5**	**23**	**0.29 ± 0.17**	**0.63±0.01**	**0.5**
COX6	3	3	29	2.56 ± 0.20	1.72 ± 0.36	1.5
DCUP	**2**	**2**	**13**	0.00 ± 0.00	**0.13 ± 0.05**	**Cntr only**
HEMO	2	2	8	0.41 ± 0.03	0.20 ± 0.09	2.0
MIC27	3	3	14	0.46 ± 0.11	0.11 ± 0.12	4.1
NLTP	4	4	9	0.87 ± 0.11	0.43 ± 0.1	2.0
NDUA7	2	2	18	0.47 ± 0.10	0.24 ± 0.04	2.0
Genetic Information Transfer						
HDGR2	8	5	12	0.40 ± 0.05	0.24 ± 0.08	1.7
RPL23A	3	3	17	1.38 ± 0.20	0.93 ± 0.07	1.5
RS26	2	2	19	0.47 ± 0.10	0.29 ± 0.03	1.6
SYRC	2	2	4	0.42 ± 0.04	0.24 ± 0.09	1.7
Ubiquitin-Proteasome System and Protein Folding						
CCD47	**2**	**2**	**9**	**0.04 ± 0.03**	**0.95 ± 0.01**	**0.4**
PSB3	**4**	**4**	**29**	**1.35 ± 0.32**	**2.02 ± 0.20**	**0.1**
PSMD6	2	2	6	0.46 ± 0.07	0.18 ± 0.05	2.4
UBE3A	**2**	**2**	**4**	**0.09 ± 0.01**	**0.26 ± 0.05**	**0.4**
Cell Survival and Signaling						
CPNE3	4	3	11	0.48 ± 0.09	0.25 ± 0.05	1.9
MANF	**2**	**2**	**18**	**0.38 ± 0.1**	**0.59± 0.06**	**0.7**
MLF2	2	2	11	0.37 ± 0.08	0.15 ± 0.08	2.4
SH3L1	3	3	38	1.19 ± 0.11	0.61 ± 0.27	2.0

Table 2.

Retinal proteins with differential abundance (≥1.5-fold) in the HPCD-treated (Tx) *vs* control (Cntr) *Cyp27a1*$^{-/-}$*Cyp46a1*$^{-/-}$ mice. Protein grouping is by process and shows each protein only in one group despite the involvement in multiple processes. Proteins with a decreased expression are in bold.

Protein	№ of Peptides with Significant Changes in Abundance	№ of Unique Peptides	Sequence Coverage (%)	Peptide Intensity (a.u.) × 10^6		Tx/Cntr, Protein Ratio
				Tx	Cntr	
Protein Folding						
CRBA1	11	11	78	6.73 ± 2.26	1.24± 0.86	5.4
CRBA2	8	8	57	3.59 ± 1.21	0.52 ± 0.36	7.0
CRBA4	4	4	34	1.26 ± 0.45	0.00 ± 0.00	Tx only
CRBB1	9	9	54	3.08 ± 1.07	0.41± 0.19	7.5
CRBB2	14	14	74	30.2 ± 8.88	5.29 ± 2.96	5.7
CRBB3	7	7	46	2.09 ± 0.94	0.17 ± 0.19	12.5
CRGB	12	3	68	2.82 ± 1.07	0.17 ± 0.15	16.7
CRGC	11	4	63	2.01 ± 0.91	0.05± 0.08	40.9
CRGD	8	3	51	3.07 ± 1.3	0.10 ± 0.11	29.5
CRYAA	14	14	47	32.30 ± 8.85	6.23 ± 3.25	5.2
CRYAB	11	11	54	7.97 ± 2.41	1.05 ± 0.71	7.6
CRYGS	7	7	65	10.68 ± 5.21	1.32 ± 0.62	8.1
Vesicular Transport and Cytoskeletal Organization						
ARFG1	3	3	21	0.56 ± 0.19	0.12±0.11	4.8
DMXL2	**20**	**19**	**14**	**0.37 ± 0.15**	**0.81± 0.06**	**0.5**
IQEC3	2	2	4	0.21 ± 0.05	0.11 ± 0.01	1.9
KI21B	**3**	**2**	**3**	**0.15 ± 0.07**	**0.41 ± 0.11**	**0.4**
PP2BB	5	2	14	0.29 ± 0.05	0.005 ± 0.01	61.7
RCN2	18	18	79	6.89 ± 0.75	4.37 ± 0.98	1.6
S4A7	5	5	12	0.75 ± 0.11	0.43 ± 0.15	1.8
SNTB1	2	2	6	0.28 ± 0.03	0.11 ± 0.04	2.5
THOP1	5	5	13	0.99 ± 0.16	0.61 ± 0.16	1.6
Metabolism and Energy Homeostasis						
ACSF2	3	2	6	0.14 ± 0.03	0.08 ± 0.01	1.7
CAH3	6	6	38	1.31 ± 0.71	0.04 ± 0.07	31.7
CDS2	5	4	10	1.10 ± 0.15	0.71 ± 0.08	1.6
FABP5	4	4	39	1.29 ± 0.26	0.56 ± 0.10	2.3
MAT2B	**2**	**2**	**7**	**0.13 ± 0.02**	**0.36 ± 0.10**	**0.4**
Genetic Information Transfer						
H32	21	7	55	27.04 ± 6.18	13.67 ± 3.04	2.0
SMCA5	**4**	**4**	**5**	**0.19 ± 0.05**	**0.42 ± 0.05**	**0.5**
TE2IP	4	3	17	0.50 ± 0.05	0.32 ± 0.05	1.6
TMEM201	2	2	4	0.07 ± 0.04	0.006 ± 0.01	12.8
XPO5	3	3	6	0.33 ± 0.05	0.06 ± 0.11	5.0